Int J Thermophys (2009) 30:883–909
DOI 10.1007/s10765-009-0591-5

Estimation of Density as a Function of Temperature and Pressure for Imidazolium-Based Ionic Liquids Using a Multilayer Net with Particle Swarm Optimization

Juan A. Lazzús

Received: 18 August 2008 / Accepted: 11 May 2009 / Published online: 28 May 2009

Abstract The liquid density of imidazolium-based ionic liquids has been estimated using a combined method that includes an artificial neural network and a simple group contribution method. A total of 1736 data points of density at several temperatures and pressures, corresponding to 131 ionic liquids, have been used to train the neural network developed with particle swarm optimization. To discriminate among the different substances, the molar mass and the structure of the molecule were given as input variables. Then, new values of density as a function of temperature and pressure for 33 other ionic liquids (426 data points) have been predicted and the results compared to experimental data from the literature. The results show that the chosen artificial neural network with particle swarm optimization and the group contribution method represent an excellent alternative for the estimation of the liquid density of imidazolium-based ionic liquids with acceptable accuracy ($AARD = 0.44$; $R^2 = 0.9934$), for a wide range of temperatures and pressures (258 K to 393 K and 99 kPa to 206,940 kPa).

Keywords Artificial neural networks · Group contribution method · Ionic liquids · Liquid density · Particle swarm optimization

1 Introduction

Ionic liquids (ILs) have been the object of increasing attention due to their unique physicochemical properties such as high thermal stability, large liquidus range, high ionic conductivity, high solvating capacity, negligible vapor pressure, and nonflammability that make them ideal solvents for green chemistry and clean synthesis [1]. ILs are organic salts composed of cations and anions that are liquid at conditions around

J. A. Lazzús (✉)
Departamento de Física, Universidad de La Serena, Casilla 554, La Serena, Chile
e-mail: jlazzus@dfuls.cl

room temperature [2]. The most commonly used cation in room-temperature ionic liquids (RILs) is dialkylimidazolium [3]. Moreover, in recent years, 1-alkyl-3-methylimidazolium ($[C_n mim]^+$) ILs have been intensively studied [4].

The liquid density (ρ) is probably the most measured property of ILs [5,6]. One reason is that its determination is straightforward and can be very accurate if the appropriate equipment, usually a pycnometer or densimeter, is used [7,8]. Density is a physical property required in several design problems and in liquid metering calculations [5,9]. The reported densities of ILs vary between $1.12\,g \cdot cm^{-3}$ and $2.4\,g \cdot cm^{-3}$ [5,7].

Imidazolium-based ionic liquids (MIM-ILs) have some special characteristics that make them suitable for uses in bioprocesses [10]. The design of equipment such as condensers, reboilers, liquid/liquid two-phase mixer-settler units, sizing of storage vessels, calculation of tower heights, and material and energy balances involving liquids and vapor–liquid and liquid–liquid separation processes, all require accurate values of liquid density [5].

There exist a great variety of analytical expressions that allow correlation and prediction of the density of liquids. Such expressions are usually based on the use of adjustable parameters for each fluid (correlations), on the corresponding-states principle, and on semi-empirical and predictive methods with the group contribution method (GCM) [5].

Among the classical proposals presented in the literature, the approach developed by Lydersen [11] is perhaps the most widely used GCM to estimate critical properties. Later, Joback and Reid [12] developed a method that is frequently mentioned in the literature and used in several applications. In all these methods, the property of a compound is calculated by summing up the contributions of certain defined groups of atoms, considering at the same time the number frequency of each group occurring in the molecule.

Several authors use these concepts of GCM to calculate the density of diverse substances [13–18]; however, in these works, the authors do not incorporate ILs. Recently, Ye and Shreeve [19] proposed a group activity method for the estimation of densities of RILs and salts. They estimated the density of a small range of ILs with good accuracy, but its application is restricted to 298.15 K and atmospheric pressure. Gardas and Coutinho [9] proposed an extension of the Ye and Shreeve GCM [19] for the estimation of densities of ILs. The new version presented allows the estimation of densities in wide ranges of temperature and pressure, but only for a small range of ILs.

Concerning the computational applications to the study of ILs, several publications demonstrate the general suitability of these methods to calculate several properties. Palomar and co-workers [6] predicted the specific density and molar liquid volume of 40 imidazolium-based ionic liquids at 298 K using the COSMO-RS method.

The aforementioned group contribution methods use linear and nonlinear regression techniques to represent the relations among the variables of a given system. The relationship between the physical and thermodynamic properties is highly nonlinear, and consequently an artificial neural network (ANN) can be a suitable alternative to model the underlying thermodynamic properties. ANN is an especially efficient algorithm to approximate any function with a finite number of discontinuities by learning

the relationships between input and output vectors [20]. Thus, ANN is an appropriate technique to model the nonlinear behavior of thermophysical properties [5,21].

Taskinen and Yliruusi [22] presented a complete list of properties that have been analyzed in the literature using different approaches of artificial neural networks. Properties such as boiling point, critical temperature, critical pressure, vapor pressure, heat capacity, enthalpy of sublimation, heat of vaporization, density, surface tension, viscosity, thermal conductivity, and acentric factor, among others, were thoroughly reviewed. Applications of neural networks to mixture properties (PTV properties, vapor–liquid equilibrium, activity coefficients) have been also presented in other publications [23,24]. To the best of the author's knowledge, there is no application for liquid density as a function of the temperature and pressure, $\rho(T, P)$, such as the one presented here, and certainly there is no publication on the prediction of these properties for imidazolium-based ILs using ANN.

In this work $\rho(T, P)$ of MIM-ILs has been correlated and predicted using a simple GCM implemented in an ANN replacing standard backpropagation with particle swarm optimization (PSO), which is one of the most recently developed evolutionary algorithms [25].

2 Neural Network Used

Many models of neural networks have been used in the estimate of thermodynamic properties [26–28]. In this work, a typical three-layer feedforward neural network was used, which is very effective for representing nonlinear relationships among variables. The network was programmed with the software MATLAB Version 6.5.0 [29] and consists of an input layer, a hidden layer, and an output layer, connected by weight and bias that quantify the influence of each fact and of each variable. There are two main states in the operation of a neural network: the learning and the validation. The learning or training is the process for which a neural network modifies the weights in answer to entrance information [5,21,24].

This ANN program considers the reading of the necessary data organized in an Excel file: $\rho(T, P)$ experimental data of MIM-ILs are used to train the network. To distinguish between the different physical and chemical properties of the substances considered in this study, so the network can discriminate and learn in optimum form, the following properties are considered: the molecular mass M (size) and the structure of the molecules, represented by the number of well-defined groups forming the molecule, are provided as variables.

The input layer contains one neuron (node) for each variable. The output layer has one node generating the scaled estimated value of the ρ. The number of hidden neurons needs to be sufficient to ensure that the information contained in the data utilized for training the network is adequately represented. There is no specific approach to determine the number of neurons of the hidden layer; many alternative combinations are possible. The optimum number of neurons was determined by adding neurons in systematic form during the learning process. The ANN was trained with particle swarm optimization [30]. Some researchers have used PSO to train neural networks

and found that PSO-based ANN has a better training performance, faster convergence rate, and a better predicting ability than the standard backpropagation algorithm [31].

PSO is a population-based optimization tool, where the system is initialized with a population of random particles and the algorithm searches for optima by updating generations [32]. In a PSO system, each particle is "flown" through the multidimensional search space, adjusting its position in search space according to its own experience and that of neighboring particles. The particle therefore makes use of the best position encountered by itself and that of its neighbors to position itself toward an optimal solution. The performance of each particle is evaluated using a predefined fitness function, which encapsulates the characteristics of the optimization problem [31].

In each iteration, the velocity for each particle is calculated according to the following formula:

$$v_i(t+1) = wv_i(t) + \alpha_i\,(p_i - x_i(t)) + \alpha_2\,(p_G - x_i(t)) \tag{1}$$

where t is the current step number, w is the inertia weight, α_1 and α_2 are the acceleration constants, $x_i(t)$ is the current position of the particle, p_i is the best solution that this particle has reached, and p_G is the best solution that all the particles have reached. In general, the value of each component in v can be restricted to the range $[-v_{max}, v_{max}]$ to control excessive roaming of particles outside the search space [32]. After calculating the velocity, the new position of every particle is

$$x_i(t+1) = x_i(t) + v_i(t+1) \tag{2}$$

The PSO algorithm performs repeated applications of the update equations above until a specified number of iterations have been exceeded, or until the velocity updates are close to zero.

The total steps to calculate the output parameter (ρ), using the input parameters, were as follows [5,21,24]:

The net inputs (N) are calculated for the hidden neurons coming from the input neurons. For a hidden neuron

$$N_j^h = \sum_i^n w_{ij}^h p_i + b_j^h \tag{3}$$

where p corresponds to the vector of the inputs of the training, j is the hidden neuron, w_{ij} is the weight of the connection among the input neurons with the hidden layer, and the term b_j corresponds to the bias of the neuron j of the hidden layer, reached in its activation. Starting from these inputs, the outputs (y) of the hidden neurons are calculated, using a transfer function f^h associated with the neurons of this layer;

$$y_j^h = f_j^h\left(\sum_i^n w_{ij}^h p_i + b_j^h\right) \tag{4}$$

Similar calculations are carried out to obtain the results of each neuron of the following layer until the output layer is reached.

To minimize the error, the transfer function f should be differentiable. In the ANN, two types of transfer functions were used: the hyperbolic tangent function (*tansig*) in the hidden layer, defined by the equation

$$f\left(N_{jk}\right) = \frac{e^{N_{jk}} - e^{-N_{jk}}}{e^{N_{jk}} + e^{-N_{jk}}} \tag{5}$$

and the linear function (*purelin*) in the output layer, defined as

$$f\left(N_{jk}\right) = \left(N_{jk}\right) \tag{6}$$

All the neurons of the ANN have an associated activation value for a given input pattern, and the algorithm continues finding the error that is presented for each neuron, except those of the input layer. After finding the output values, the weights of all layers of the network are actualized by PSO, using Eqs. 1 and 2.

Figure 1 presents a block diagram of the program developed and written in MatLab M-file.

3 Data Used and Training

In this study, 1736 experimental data points for 131 MIM-ILs were used to train the ANN + PSO, introducing as entrance parameters temperature (T), pressure (P), molecular mass (M), and the structural groups that form the molecules. The output parameter is the liquid density (ρ). Table 1 shows the 30 groups used as entrance variables. The value associated to the structural group was defined as: 0, when the group does not appear in the substance and n, when the group appears n times in the substance. For instance, for 1-propyl-3-methylimidazolium hexafluorophosphate, besides the data points (T, P), the property data are $M = 270.2\,\mathrm{kg \cdot kmol^{-1}}$ and the structure of the molecule [–CH3]=2, [–CH2–]=2, [=CH-(ring)]=3, [>N-(ring)]=1, [=N-(ring)]=1, [–P]=1, and [–F]=6. Table 2 shows the properties for all ILs considered in the study. The heterogeneous set of MIM-ILs includes cations of mono-, di-, and tri-imidazolium and anions such as halides, pseudohalides, sulfates, sulfonates, tosylates, imides, amides, borates, phosphates, carboxylates, triflates, trifluoracetates, and metal complexes.

All data chosen correspond to those claimed by the authors as being experimentally determined. Data available in the literature obtained from theoretical methods, correlations, or extrapolations of any kind were not considered. Also, data for which the authors themselves indicate that accuracy is not guaranteed for any reason (presence of impurities, instability of the fluid, or problems with the equipment) were not considered.

As seen in Table 2, $\rho(T, P)$ properties cover wide ranges: 273 K to 393 K for the temperature, 99 kPa to 206,940 kPa for the pressure, and $983\,\mathrm{kg \cdot m^{-3}}$ to $2,151\,\mathrm{kg \cdot m^{-3}}$ for ρ. In addition, the ILs included in the study have very different physical and

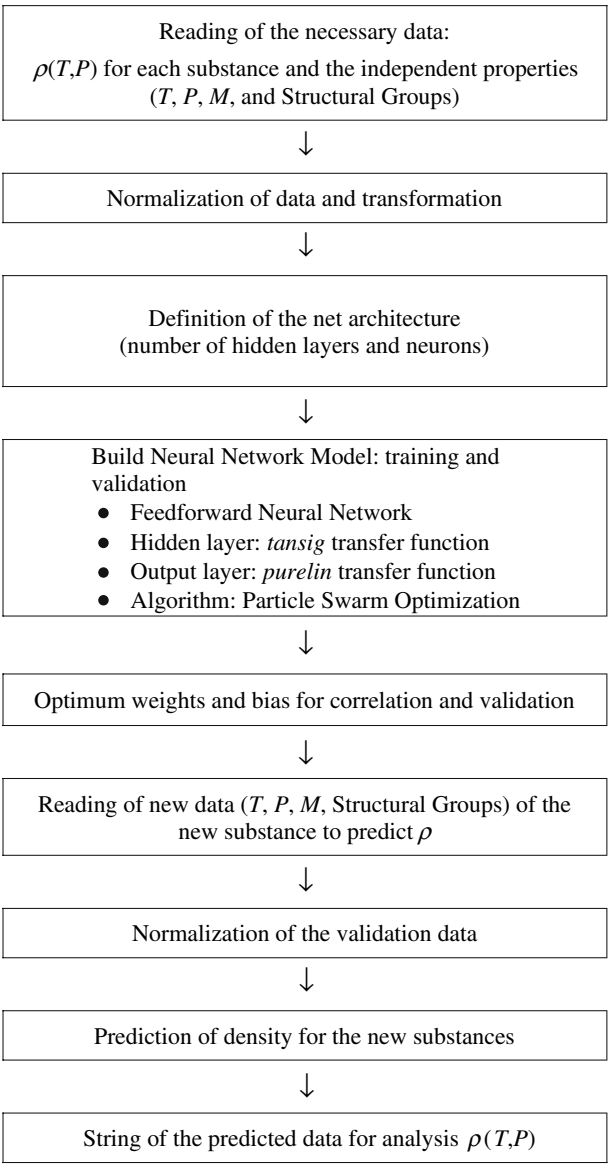

Fig. 1 Flow diagram for the ANN+PSO program developed for this work

chemical characteristics. Low molecular mass substances such as 1-methylimidazolium chloride ($M = 119$) to high molecular mass substances such as [C9(bim)2][dTf2N], with $M = 935$, were considered. Thus, the problem is not straightforward and probably is one of the reasons why the liquid density for MIM-ILs has not been treated using ANN as proposed in this paper.

Table 1 Groups considered in the ANN method for MIM-ILs

Structural groups	
Non-ring	–S– [>S–]$^+$ [> S <]$^+$
–CH_3	–SO_2–
–CH_2–	–BH
>CH–	–Al
>C< [>C–]$^-$	–Ga
–OH	–In
–O– [–O]$^-$	–Fe
–COO–	With ring
[–N–]$^-$ >N– [> N <]$^+$	=CH–
–CN	>C<
–NO_2	=C<
–F [–F]$^-$	–O–
–Cl [–Cl]$^-$	>C=O
–Br	–NH–
–P [>P–]$^+$ [>P<]$^+$	>N– [> N <]$^+$
–B	–N= [> N =]$^+$

This work used a leave-20 %-out cross-validation method to estimate the predictive capabilities of the model [5]. Training and prediction sets were selected randomly, with the consideration that in the group contribution methods, the molecules are decomposed into fragments and all fragments that are present with adequate frequency are in the training database.

Once the training was successfully done and the optimum network architecture was determined, new input data (T, P, M, and structural groups) of 33 ionic liquids (426 data points) not used in the training process were fed to the ANN and the liquid density was predicted at several temperatures and pressures.

Several network architectures were tested to select the most accurate scheme. Since no additional information about the recommended number of neurons has been found for the calculation of properties for any type of substances, the optimum number of neurons was determined by trial and error [5,24]. Figure 2 shows the average absolute relative deviation ($AARD$) found in correlating ρ of all MIM-ILs as a function of the number of neurons in the hidden layer. As observed in the figure, the optimum number of neurons in the hidden layer is between 5 and 7. The network that gave the lowest deviation during training was one with 33 parameters in the input layer, 6 neurons in the hidden layer, and one neuron in the output layer. For this architecture, the average deviation during training is 0.43 % and during prediction is 0.49 %.

The accuracy of the chosen final network was checked using the $AARD$ between the calculated value (calc) of ρ and the experimental data (exp) from the literature. The deviations were calculated as:

$$AARD = \frac{100}{N}\sum_{i=1}^{N}\left|\frac{\rho^{\text{calc}} - \rho^{\text{exp}}}{\rho^{\text{exp}}}\right|_i \tag{7}$$

Table 2 Imidazolium-based ionic liquids, properties, and deviations used in the ANN+PSO model during training and prediction

IUPAC name	Abbreviation	Formula	T (K)	P (kPa)	M	ρ (kg · m^{-3})	No. data	*AARD*	Ref.
Training Set									
1-methylimidazolium chloride	[mim] [Cl]	$C_4H_7N_2Cl$	353	101	118.6	1183	1	0.01	[33]
1-methylimidazolium hydrogen sulfate	[mim] [HSO4]	$C_4H_8N_2SO_4$	298	101	179.3	1484	1	0.00	[33]
1-ethyl-3-methylimidazolium tetrachloroaluminate	[emim][AlCl4]	$C_6H_{11}N_2AlCl_4$	298	101	280.0	1294	1	0.32	[34]
1-ethyl-3-methylimidazolium tetrafluoroborate	[emim] [BF4]	$C_6H_{11}N_2BF_4$	298–308	101	198.0	1280–1272	9	1.18	[35]
1-ethyl-3-methylimidazolium tetrafluoroborate	[emim] [BF4]	$C_6H_{11}N_2BF_4$	293–393	100–30000	198.0	1318–1230	96	0.29	[36]
1-ethyl-3-methylimidazolium chloride	[emim] [Cl]	$C_6H_{11}N_2Cl$	295	101	146.6	1186	1	2.51	[33]
1-ethyl-3-methylimidazolium chlorogallate	[emim] [GaCl4]	$C_6H_{11}N_2GaCl_4$	288–343	101	322.7	1479–1436	11	0.15	[37]
1-ethyl-3-methylimidazolium indium choride	[emim] [InCl4]	$C_6H_{11}N_2InCl_4$	293–343	101	367.8	1641–1591	11	0.14	[38]
methyloxymethyl-3-methylimidazolium tetrafluoroborate	[mommim] [BF4]	$C_6H_{11}N_2OBF_4$	298	101	214.0	1330	1	0.32	[39]
methyloxymethyl-3-methylimidazolium hexafluorophosphate	[mommim] [PF6]	$C_6H_{11}N_2OPF_6$	298	101	272.1	1480	1	0.08	[39]
1-ethyl-3-methylimidazolium hydrogen sulfate	[emim] [HSO4]	$C_6H_{12}N_2SO_4$	298	101	207.4	1367	1	0.02	[33]
1,3-dimethylimidazolium methyl sulfate	[dmim] [MSO4]	$C_6H_{12}N_2SO_4$	293–303	101	208.2	1331–1324	3	0.31	[40]
1,3-dimethylimidazolium methyl sulfate	[dmim] [MSO4]	$C_6H_{12}N_2SO_4$	283–343	101	208.2	1338–1296	13	0.16	[41]
1,3-dimethylimidazolium bis[(trifluoromethyl)sulfonyl]imide	[dmim] [Tf2N]	$C_7H_9N_3F_6S_2O_4$	298–353	101	377.3	1570–1514	12	0.14	[5]
1-ethyl-3-methylimidazolium trifluoromethanesulfonate	[emim][TfO]	$C_7H_{11}N_2F_3SO_3$	298	101	260.2	1385	1	0.58	[42]
1-ethyl-3-methylimidazolium trifluoromethanesulfonate	[emim][TfO]	$C_7H_{11}N_2F_3SO_3$	295	101	260.2	1390	1	0.78	[33]
1-propyl-3-methylimidazolium tetrachloroaluminate	[prmim][AlCl4]	$C_7H_{13}N_2AlCl_4$	298	101	294.0	1262	1	0.09	[38]
1-propyl-3-methylimidazolium tetrafluoroborate	[prmim][BF4]	$C_7H_{13}N_2BF_4$	298	101	212.0	1240	1	0.32	[39]
ethyloxymethyl-3-methylimidazolium tetrafluoroborate	[moemim] [BF4]	$C_7H_{13}N_2OBF_4$	298	101	228.0	1260	1	0.59	[39]
ethoxymethyl-3-methylimidazolium hexafluorophosphate	[eommim] [PF6]	$C_7H_{13}N_2OPF_6$	298	101	286.2	1400	1	0.27	[39]
1-propyl-3-methylimidazolium hexafluorophosphate	[prmim][PF6]	$C_7H_{13}N_2PF_6$	293	101	270.2	1333	1	5.31	[33]
1,3-dimethylimidazolium dimethylphosphate	[dmim] [DMPO4]	$C_7H_{15}N_2PO_4$	303	101	222.2	1253	1	0.12	[33]
1-ethyl-3-methylimidazolium hexabromide-1-carbon icosahedral	[emim] [CB11H6Br6]	$C_7H_{17}N_2B_{11}Br_6$	298	101	727.6	2151	1	0.01	[43]

Table 2 Continued

IUPAC name	Abbreviation	Formula	T (K)	P (kPa)	M	ρ (kg · m^{-3})	No. data	*AARD*	Ref.
1-ethyl-3-methylimidazolium hexachloride-1-carbon icosahedral	[emim] [CB11H6Cl6]	$C_7H_{17}N_2B_{11}Cl_6$	298	101	460.9	1431	1	0.00	[43]
1-ethyl-3-methylimidazolium methylcarbonicosahedral	[emim][MeCB11]	$C_7H_{25}N_2B_{11}$	298	101	256.2	1036	1	0.09	[43]
1-ethyl-3-methylimidazolium ethylcarbonicosahedral	[emim][EtCB11]	$C_7H_{27}N_2B_{11}$	298	101	270.2	1050	1	0.08	[43]
1-trifluoroethyl-3-methylimidazoli-umbis[(trifluoromethyl)sulfo-nyl]imide	[tfemim] [Tf2N]	$C_8H_8N_3F_9S_2O_4$	293	101	431.3	1660	1	0.27	[44]
1-trifluoroethyl-3-methylimidazoli-umbis[(trifluoromethyl)sulfo-nyl]imide	[tfemim] [Tf2N]	$C_8H_8N_3F_9S_2O_4$	293	101	445.3	1660	1	0.30	[44]
1-trifluoroethyl-3-methylimidazoli-umbis[(trifluoromethyl)sulfo-nyl]imide	[tfemim] [Tf2N]	$C_8H_8N_3F_9S_2O_4$	295	101	445.3	1656	1	0.23	[33]
1-ethyl-3-methylimidazolium trifluoroacetate	[emim] [ta]	$C_8H_{11}N_2F_3O_2$	298	101	224.2	1390	1	4.14	[33]
1-ethyl-3-methylimidazolium trifluoroacetate	[emim] [ta]	$C_8H_{11}N_2F_3O_2$	295	101	224.2	1285	1	3.67	[33]
1-ethyl-3-methylimidazoliumbis[(tri-fluoromethyl)sulfonyl]imide	[emim] [Tf2N]	$C_8H_{11}N_3F_6S_2O_4$	293–393	100–30000	391.3	1547–1424	96	0.06	[36]
1-ethyl-3-methylimidazolium dicyanamide	[emim] [dca]	$C_8H_{11}N_5$	298	101	177.2	1060	1	0.43	[33]
1-ethyl-3-methylimidazolium1,1,2,2-tetrafluoroethanesulfonate	[emim] [TFES]	$C_8H_{12}N_2F_4SO_3$	301	101	292.3	1502	1	0.10	[33]
1-methyl-3-ethyl-4-methylimidazoli-umbis[(trifluoromethyl)sulfo-nyl]imide	[memim] [Tf2N]	$C_8H_{12}N_3F_6S_2O_4$	293	101	392.3	1470	1	1.27	[33]

Table 2 Continued

IUPAC name	Abbreviation	Formula	T (K)	P (kPa)	M	ρ (kg · m^{-3})	No. data	*AARD*	Ref.
1,3-diethylimidazolium trifluoromethanesulfonate	[deim][TfO]	$C_8H_{13}N_2F_3SO_3$	295	101	274.3	1330	1	0.43	[33]
1-ethyl-3,5-dimethylimidazolium trifluoromethanesulfonate	[edmim] [TfO]	$C_8H_{13}N_2F_3SO_3$	295	101	274.3	1334	1	2.71	[33]
1-ethyl-3-methylimidazolium acetate	[emim] [Ac]	$C_8H_{14}N_2O_2$	298	101	170.2	1027	1	2.02	[33]
1-butyl-3-methylimidazolium tetrachloroaluminate	[bmim][AlCl4]	$C_8H_{15}N_2AlCl_4$	298	101	308.0	1243	1	0.14	[33]
1-butyl-3-methylimidazolium tetrafluoroborate	[bmim] [BF4]	$C_8H_{15}N_2BF_4$	278–303	100	226.0	1219–1201	6	0.47	[45]
1-butyl-3-methylimidazolium tetrafluoroborate	[bmim] [BF4]	$C_8H_{15}N_2BF_4$	298–333	100–60000	226.0	1230–1181	20	0.11	[45]
1-butyl-3-methylimidazolium tetrafluoroborate	[bmim] [BF4]	$C_8H_{15}N_2BF_4$	298–308	101	226.0	1202–1195	18	0.11	[35]
1-butyl-3-methylimidazolium tetrafluoroborate	[bmim] [BF4]	$C_8H_{15}N_2BF_4$	293–393	100–10000	226.0	1211–1136	77	0.14	[1]
1-butyl-3-methylimidazolium tetrafluoroborate	[bmim] [BF4]	$C_8H_{15}N_2BF_4$	298–323	101	226.0	1202–1185	6	0.17	[5]
1-butyl-3-methylimidazolium tetrafluoroborate	[bmim] [BF4]	$C_8H_{15}N_2BF_4$	293–303	101	226.0	1206–1372	38	0.12	[46]
1-butyl-3-methylimidazolium chloride	[bmim] [Cl]	$C_8H_{15}N_2Cl$	298	101	174.7	1080	1	0.58	[39]
1-butyl-3-methylimidazolium iron chloride	[bmim] [FeCl4]	$C_8H_{15}N_2FeCl_4$	283–343	101	336.9	1375–1336	13	0.10	[47]
1-butyl-3-methylimidazolium chlorogallate	[bmim] [GaCl4]	$C_8H_{15}N_2GaCl_4$	298	101	350.8	1417	1	0.52	[5]
1-butyl-3-methylimidazolium indium choride	[bmim] [InCl4]	$C_8H_{15}N_2InCl_4$	298	101	395.9	1556	1	0.32	[48]
1-butyl-3-methylimidazolium hexafluorophosphate	[bmim][PF6]	$C_8H_{15}N_2PF_6$	313–333	101	284.2	1346–1330	3	0.20	[49]
1-butyl-3-methylimidazolium hexafluorophosphate	[bmim][PF6]	$C_8H_{15}N_2PF_6$	298–323	101	284.2	1368–1339	6	0.04	[50]

Table 2 Continued

IUPAC name	Abbreviation	Formula	T (K)	P (kPa)	M	ρ (kg · m^{-3})	No. data	*AARD*	Ref.
1-butyl-3-methylimidazolium hexafluorophosphate	[bmim][PF6]	$C_8H_{15}N_2PF_6$	283–343	101	284.2	1380–1330	14	0.42	[5]
1-butyl-3-methylimidazolium hexafluorophosphate	[bmim][PF6]	$C_8H_{15}N_2PF_6$	278–343	101	284.2	1384–1330	14	0.34	[51]
1-butyl-3-methylimidazolium hexafluorophosphate	[bmim][PF6]	$C_8H_{15}N_2PF_6$	293–303	101	284.2	1372–1363	3	0.18	[40]
1-butyl-3-methylimidazolium hexafluorophosphate	[bmim][PF6]	$C_8H_{15}N_2PF_6$	283–323	101	284.2	1379–1345	9	0.15	[52]
1-butyl-3-methylimidazolium hexafluorophosphate	[bmim][PF6]	$C_8H_{15}N_2PF_6$	298–323	99–202110	284.2	1438–1340	14	0.30	[53]
1-butyl-3-methylimidazolium hexafluorophosphate	[bmim][PF6]	$C_8H_{15}N_2PF_6$	298–343	101	284.2	1360–1324	6	0.04	[53]
1-butyl-3-methylimidazolium nitrate	[bmim] [NO3]	$C_8H_{15}N_3O_2$	313–333	101	201.2	1149–1136	3	0.07	[49]
1-butyl-3-methylimidazolium hydrogen sulfate	[bmim] [HSO4]	$C_8H_{16}N_2SO_4$	298	101	235.4	1277	1	0.00	[33]
1-ethyl-3-methylimidazolium ethylsulfate	[emim] [SE]	$C_8H_{16}N_2SO_4$	313–333	101	236.3	1225–1213	3	0.25	[49]
1-ethyl-3-methylimidazolium ethylsulfate	[emim] [SE]	$C_8H_{16}N_2SO_4$	288–343	101	236.3	1244–1208	12	0.26	[54]
1-ethyl-3-methylimidazolium ethylsulfate	[emim] [SE]	$C_8H_{16}N_2SO_4$	278–348	101	236.3	1251–1204	8	0.30	[55]
1,3-dimethylimidazolium methoxyethylsulfate	[dmim] [MOESO4]	$C_8H_{16}N_2SO_5$	298	101	252.3	1314	1	3.94	[33]
1-ethyl-2,3-dimethylimidazolium hexachloride-1-carbon icosahedral	[edmim] [CB11H6Cl6]	$C_8H_{19}N_2B_{11}Cl_6$	298	101	474.9	1439	1	0.05	[43]
1-ethyl-2,3-dimethylimidazolium 1-carbon icosahedral	[edmim] [CB11H12]	$C_8H_{25}N_2B_{11}$	298	101	268.2	1072	1	0.02	[43]

Table 2 Continued

IUPAC name	Abbreviation	Formula	T (K)	P (kPa)	M	ρ (kg · m^{-3})	No. data	*AARD*	Ref.
1,3-diethylimidazolium trifluoroacetate	[deim] [ta]	$C_9H_{13}N_2F_3O_2$	295	101	238.2	1250	1	0.86	[33]
1-ethyl-2,3-dimethylimidazolium bis[(trifluoromethyl)sulfonyl]imide	[edmim] [Tf2N]	$C_9H_{13}N_3F_6S_2O_4$	298–353	101	405.3	1487–1437	10	0.10	[5]
1,3-diethylimidazolium bis[(trifluoromethyl)sulfonyl]imide	[deim] [Tf2N]	$C_9H_{13}N_3F_6S_2O_4$	295	101	405.3	1452	1	2.03	[33]
1-propyl-3-methylimidazolium-bis[(trifluoromethyl)sulfonyl]imide	[prmim] [Tf2N]	$C_9H_{13}N_3F_6S_2O_4$	298	101	405.3	1475	1	3.88	[39]
ethoxymethyl-3-methylimidazolium bis[(trifluoromethyl)sulfonyl]imide	[eomim] [Tf2N]	$C_9H_{13}N_3F_6S_2O_5$	298	101	421.3	1496	1	0.38	[39]
1-butyl-3-methylimidazolium thiocyanate	[bmim] [SCN]	$C_9H_{15}N_3S$	293–393	100–30000	197.3	1064–987	96	0.10	[36]
1,2-dimethyl-3-ethylimidazolium bis[(trifluoromethyl)sulfonyl]imide	[dmeim] [Tf2N]	$C_9H_{16}N_3F_6S_2O_4$	293	101	392.3	1510	1	1.41	[44]
1-pentyl-3-methylimidazolium tetrachloroaluminate	[pmim] [AlCl4]	$C9H_{17}N_2AlCl_4$	273–343	101	322.0	1231–1182	15	0.11	[56]
1-butyl-2,3-dimethylimidazolium tetrafluoroborate	[bdmim] [BF4]	$C_9H_{17}N_2BF_4$	300	101	240.1	1094	1	4.07	[33]
1-pentyl-3-methylimidazolium bromide	[pmim] [Br]	$C_9H_{17}N_2Br$	298	101	233.2	1262	1	1.30	[57]
1-butyl-2,3-dimethylimidazolium bis[(trifluoromethyl)sulfonyl]imide	[bdmim] [Tf2N]	$C_9H_{17}N_2Cl$	298	101	433.4	1420	1	1.32	[33]
1-pentyl-3-methylimidazolium chlorogallate	[pmim] [GaCl4]	$C_9H_{17}N_2GaCl4$	308–343	101	364.8	1368–1340	8	0.17	[56]
1-pentyl-3-methylimidazolium chloroindium	[pmim] [InCl4]	$C9H_{17}N_2InCl_4$	273–343	101	409.9	1534–1470	15	0.12	[56]
1-[2-(2-methoxyethoxy)ethyl]-3-methylimidazolium chloride	[moeemim] [Cl]	$C_9H_{17}N_2O_2Cl$	298	101	220.7	1140	1	1.27	[39]

Table 2 Continued

IUPAC name	Abbreviation	Formula	T (K)	P (kPa)	M	ρ (kg · m^{-3})	No. data	*AARD*	Ref.
1-[2-(2-methoxyethoxy)ethyl]-3-methyl imidazolium hexafluorophosphate	[moeemim] [PF6]	$C_9H_{17}N_2O_2PF_6$	298	101	330.2	1320	1	0.44	[39]
1-pentyl-3-methylimidazolium hexafluorphosphate	[pmim] [PF6]	$C_9H_{17}N_2PF_6$	298	101	298.2	1328	1	0.06	[57]
1-methyl-3-pentylimidazolium hexafluorophosphate	[mpim] [PF6]	$C_9H_{17}N_2PF_6$	294	101	298.2	1333	1	0.09	[33]
1-butyl-3-methylimidazolium methanesulfonate	[bmim] [mesy]	$C_9H_{18}N_2SO_3$	278–343	101	234.3	1226–1182	14	0.91	[51]
1-butyl-3-methylimidazolium methanesulfonate	[bmim] [mesy]	$C_9H_{18}N_2SO_3$	298–308	101	234.3	1208–1201	8	0.38	[35]
1-butyl-3-methylimidazolium methylsulfate	[bmim] [MSO4]	$C_9H_{18}N_2SO_4$	298	101	250.3	1212	1	1.72	[33]
1-ethyl-2,3-dimethylimidazolium ethyl sulfate	[edmim] [ESO4]	$C_9H_{18}N_2SO_4$	353	101	250.3	1197	1	0.81	[33]
1-ethyl-3-methylimidazolium bis(pentafluoroethylsulfonyl)imide	[emim] [BEI]	$C_{10}H_{11}N_3F_{10}S_2O_4$	298	101	491.3	1590	1	0.12	[33]
1-methyl-3-ethylimidazolium bis(pentafluoroethylsulfonyl)imide	[emim] [BEI]	$C_{10}H_{11}N_3F_{10}S_2O_4$	283–348	101	491.3	1608–1534	4	0.18	[58]
1-butyl-3-methylimidazolium trifluoroacetate	[bmim] [ta]	$C_{10}H_{15}N_2F_3O_2$	295	101	252.2	1209	1	0.84	[33]
1-butyl-3-methylimidazolium bis[(trifluoromethyl)sulfonyl]imide	[bmim] [Tf2N]	$C_{10}H_{15}N_3F_6S_2O_4$	298–323	101	419.4	1436–1404	6	3.14	[50]
1-isobutyl-3-methylimidazolium bis[(trifluoromethyl)sulfonyl]imide	[i-bmim] [Tf2N]	$C_{10}H_{15}N_3F_6S_2O_4$	293	101	419.4	1430	1	0.02	[44]
1-butyl-3-methylimidazolium bis[(trifluoromethyl)sulfonyl]imide	[bmim] [Tf2N]	$C_{10}H_{15}N_3F_6S_2O_4$	278–333	101	419.4	1453–1401	12	3.01	[52]

Table 2 Continued

IUPAC name	Abbreviation	Formula	T (K)	P (kPa)	M	ρ (kg · m^{-3})	No. data	*AARD*	Ref.
1-butyl-3-methylimidazolium bis[(trifluoromethyl)sulfonyl]imide	[bmim] [Tf2N]	$C_{10}H_{15}N_3F_6S_2O_4$	278–333	101	419.4	1455–1403	12	3.12	[52]
1-butyl-3-methylimidazolium bis[(trifluoromethyl)sulfonyl]imide	[bmim] [Tf2N]	$C_{10}H_{15}N_3F_6S_2O_4$	298–328	100–59100	419.4	1476–1408	168	0.86	[59]
1,2-dimethyl-3-propylimidazolium bis[(trifluoromethyl)sulfonyl]imide	[dmprim] [Tf2N]	$C_{10}H_{15}N_3F_6S_2O_4$	295–345	101	419.4	1457–1416	6	0.26	[60]
1,3-diethyl-4-methylimidazolium bis[(trifluoromethyl)sulfonyl]imide	[E1,3M4I] [Tf2N]	$C_{10}H_{15}N_3F_6S_2O_4$	295	101	419.4	1432	1	1.74	[33]
1-isobutyl-3-methylimidazolium bis[(trifluoromethyl)sulfonyl]imide	[i-bmim] [Tf2N]	$C_{10}H_{15}N_3F_6S_2O_4$	295	101	419.4	1428	1	0.02	[33]
1-propyl-2,3-dimethylimidazolium bis[(trifluoromethyl)sulfonyl]imide	[pdmim] [Tf2N]	$C_{10}H_{15}N_3F_6S_2O_4$	295	101	419.4	1457	1	0.01	[33]
1-butyl-3-methylimidazolium dicyanamide	[bmim] [dca]	$C_{10}H_{15}N_5$	297–356	101	205.3	1058–1026	6	0.49	[60]
1-butyl-3-methylimidazolium 1,1,2,2-tetrafluoroethanesulfonate	[bmim] [TFES]	$C_{10}H_{16}N_2F_4SO_3$	301	101	320.3	1324	1	1.28	[33]
1-butyl-3-ethylimidazolium trifluoromethanesulfonate	[beim] [TfO]	$C_{10}H_{17}N_2F_3SO_3$	298	101	302.3	1270	1	2.14	[33]
1-butyl-3-methylimidazolium acetate	[bmim] [Ac]	$C_{10}H_{18}N_2O_2$	298	101	198.3	1055	1	0.29	[33]
1-hexyl-3-methylimidazolium tetrafluoroborate	[hmim] [BF4]	$C_{10}H_{19}N_2BF_4$	288–323	101	254.1	1151–1127	36	0.16	[46]
1-hexyl-3-methylimidazolium chloride	[hmim] [Cl]	$C_{10}H_{19}N_2Cl$	298–343	101	202.7	1040–1014	10	0.71	[61]
1-hexyl-3-methylimidazolium chlorogallate	[hmim] [GaCl4]	$C_{10}H_{19}N_2GaCl_4$	298	101	378.8	1376	1	1.28	[56]
1-butyl-2,3-dimethylimidazolium hexachloride-1-carbon icosahedral	[bdmim] [CB11H6Cl6]	$C_{10}H_{23}N_2B_{11}Cl_6$	298	101	502.9	1367	1	0.16	[43]

Table 2 Continued

IUPAC name	Abbreviation	Formula	T (K)	P (kPa)	M	ρ (kg · m^{-3})	No. data	*AARD*	Ref.
1-p-chlorobenzyl-3-methylimidazolium chloride	[ClBenmim] [Cl]	$C_{11}H_{12}N_2Cl_2$	298	101	243.1	1267	1	0.77	[33]
1-p-fluorobenzyl-3-methylimidazolium chloride	[FBenMim] [Cl]	$C_{11}H_{12}N_2FCl$	298	101	226.7	1283	1	0.41	[33]
1-benzyl-3-methylimidazolium chloride	[Bemim] [Cl]	$C_{11}H_{13}N_2Cl$	298	101	208.7	1193	1	0.62	[33]
1-butyl-3-methylimidazolium 1,1,2,3,3,3-hexafluoropropanesulfonate	[bmim] [HFPS]	$C_{11}H_{16}N_2F_6SO_3$	283–348	101	370.3	1422–1364	4	0.53	[58]
1-butyl-3-methylimidazolium 1,1,2-trifluoro-2-(trifluoromethoxy)ethanesulfonate	[bmim] [TTES]	$C_{11}H_{16}N_2F_6SO_4$	283–348	101	386.3	1409–1345	4	0.45	[58]
1-pentyl-3-methylimidazolium bis[(trifluoromethyl)sulfonyl]imide	[pmim] [Tf2N]	$C_{11}H_{17}N_3F_6S_2O_4$	298–333	100–59590	433.4	1444–1371	165	0.12	[62]
1,3-dibutylimidazolium chloride	[dbim] [Cl]	$C_{11}H_{21}N_2Cl$	298	101	216.8	1008	1	3.11	[39]
1-hexyl-3-ethylimidazolium hexafluorophosphate	[C2C6I] [PF6]	$C_{11}H_{21}N_2PF_6$	298	101	326.3	1262	1	0.15	[39]
1-heptyl-3-methylimidazolium hexafluorophosphate	[hpmim] [PF6]	$C_{11}H_{21}N_2PF_6$	298	101	326.3	1262	1	0.14	[39]
1-ethyl-3-methylimidazolium diethylenglycolmonomethylethersulphate	[emim] [GlyMSO4]	$C_{11}H_{22}N_2SO_6$	298–313	101	310.4	1237–1226	3	0.04	[5]
1-benzyl-3-methylimidazolium trifluoromethanesulfonate	[Bemim] [TfO]	$C_{12}H_{13}N_2F_3SO_3$	303	101	322.3	1300	1	0.89	[33]
1-butyl-3-methylimidazolium heptafluorobutanoate	[bmim] [hb]	$C_{12}H_{15}N_2F_7O_2$	295	101	352.3	1333	1	0.11	[33]
1-butyl-3-methylimidazolium tris(trifluoromethylsulfonyl)methide	[bmim] [TMEM]	$C_{12}H_{15}N_2F_9S_3O_6$	298–333	101	550.4	1563–1529	5	0.04	[58]
1-butyl-3-methylimidazolium nonafluorobutanesulfonate	[bmim] [NfO]	$C_{12}H_{15}N_2F_9SO_3$	295	101	438.3	1473	1	1.91	[33]

Table 2 Continued

IUPAC name	Abbreviation	Formula	T (K)	P (kPa)	M	ρ (kg · m^{-3})	No. data	*AARD*	Ref.
1-ethyl-3-methylimidazolium nonafluorobutanesulfonate	[emim] [NfO]	$C_{12}H_{15}N_2F_9SO_3$	295	101	439.3	1473	1	0.12	[33]
1-butyl-3-methylimidazolium bis(oxalato)borate	[bmim] [BOB]	$C_{12}H_{15}N_2O_8B$	298	101	326.1	1284	1	0.00	[63]
1-butyl-3-methylimidazolium 1,1,2-trifluoro-2-(perfluoroethoxy)ethanesulfonate	[bmim] [TPES]	$C_{12}H_{16}N_2F_8SO_4$	283–348	101	436.3	1439–1372	4	1.28	[58]
1-butyl-3-methylimidazolium 2-(1,2,2,2-tetrafluoroethoxy)-1,1,2,2-tetrafluoroethanesulfonate	[bmim] [FS]	$C_{12}H_{16}N_2F_8SO_4$	283–348	101	436.3	1464–1401	4	0.63	[64]
1-octyl-3-methylimidazolium tetrafluoroborate	[omim] [BF4]	$C_{12}H_{23}N_2BF_4$	293–393	100–10000	282.1	1113–1041	77	0.05	[1]
1-octyl-3-methylimidazolium tetrafluoroborate	[omim] [BF4]	$C_{12}H_{23}N_2BF_4$	313–333	101	282.1	1080–1066	3	1.23	[49]
1-octyl-3-methylimidazolium tetrafluoroborate	[omim] [BF4]	$C_{12}H_{23}N_2BF_4$	273–363	101	282.1	1121–1060	14	0.26	[65]
1-octyl-3-methylimidazolium tetrafluoroborate	[omim] [BF4]	$C_{12}H_{23}N_2BF_4$	288–323	101	282.1	1110–1087	36	0.20	[46]
1-octyl-3-methylimidazolium tetrafluoroborate	[omim] [BF4]	$C_{12}H_{23}N_2BF_4$	298–323	99–206940	282.1	1162–1075	15	0.38	[53]
1-octyl-3-methylimidazolium tetrafluoroborate	[omim] [BF4]	$C_{12}H_{23}N_2BF_4$	298–343	101	282.1	1091–1062	6	0.98	[53]
1-octyl-3-methylimidazolium chloride	[omim] [Cl]	$C_{12}H_{23}N_2Cl$	298–343	101	230.8	1009–983	10	0.53	[61]
1-octyl-3-methylimidazolium hexafluorophosphate	[omim] [PF6]	$C_{12}H_{23}N_2PF_6$	293–393	100–10000	340.3	1248–1166	77	0.19	[1]
1-octyl-3-methylimidazolium hexafluorophosphate	[omim] [PF6]	$C_{12}H_{23}N_2PF_6$	313–333	101	340.3	1211–1197	3	0.88	[49]

Table 2 Continued

IUPAC name	Abbreviation	Formula	T (K)	P (kPa)	M	ρ (kg · m^{-3})	No. data	*AARD*	Ref.
1-octyl-3-methylimidazolium hexafluorophosphate	[omim] [PF6]	$C_{12}H_{23}N_2PF_6$	278–343	101	340.3	1252–1202	14	0.23	[51]
1-octyl-3-methylimidazolium hexafluorophosphate	[omim] [PF6]	$C_{12}H_{23}N_2PF_6$	293–303	101	340.3	1240–1230	3	0.25	[40]
1-octyl-3-methylimidazolium hexafluorophosphate	[omim] [PF6]	$C_{12}H_{23}N_2PF_6$	293–303	101	340.3	1240–1232	3	0.25	[5]
1-octyl-3-methylimidazolium hexafluorophosphate	[omim] [PF6]	$C_{12}H_{23}N_2PF_6$	298–323	99–204180	340.3	1304–1207	14	0.35	[53]
1-octyl-3-methylimidazolium hexafluorophosphate	[omim] [PF6]	$C_{12}H_{23}N_2PF_6$	298–343	101	340.3	1225–1192	6	0.64	[53]
1-(1-phenylalkyl)-3-methylimidazolium bis[(trifluoromethyl) sulfonyl] imide	[Ph(CH2)mim] [Tf2N]	$C_{13}H_{13}N_3F_6S_2O_4$	298–323	101	453.4	1491–1458	6	0.02	[50]
1-(3-phenylalkyl)-3-methylimidazolium hexafluorophosphate	[Ph(CH2)3mim] [PF6]	$C_{13}H_{17}N_2PF_6$	298	101	346.3	1407	1	0.01	[50]
1-heptyl-3-methylimidazolium bis[(trifluoromethyl)sulfonyl]imide	[hpmim] [Tf2N]	$C_{13}H_{21}N_3F_6S_2O_4$	293–393	100–30000	461.5	1374–1262	96	0.12	[36]
1-octyl-3-methylimidazolium trifluoromethanesulfonate	[omim] [TfO]	$C_{13}H_{23}N_2F_3SO_3$	298	101	344.4	1120	1	6.58	[66]
1-octyl-3-ethylimidazolium hexafluorophosphate	[C2C8I] [PF6]	$C_{13}H_{25}N_2PF_6$	298	101	354.3	1212	1	1.16	[39]
1-octyl-3-methylimidazolium hexachloride-1-carbon icosahedral	[omim] [CB11H6Cl6]	$C_{13}H_{28}N_2B_{11}Cl_6$	298	101	545.0	1341	1	0.14	[43]
1-(2-phenylalkyl)-3-methylimidazolium bis[(trifluoromethyl) sulfonyl] imide	[Ph(CH2)2mim] [Tf2N]	$C_{14}H_{15}N_3F_6S_2O_4$	298	101	467.4	1470	1	0.25	[50]

Table 2 Continued

IUPAC name	Abbreviation	Formula	T (K)	P (kPa)	M	ρ (kg · m^{-3})	No. data	$AARD$	Ref.
1-(n-butyl)-1,3'-dimethyl-2,2'-biimidazolium dicyanamide	[BM2I] [dca]	$C_{14}H_{19}N_7$	298	101	285.4	1055	1	0.01	[5]
1-octyl-3-methylimidazolium bis[(trifluoromethyl)sulfonyl]imide	[omim] [Tf2N]	$C_{14}H_{23}N_3F_6S_2O_4$	293–393	100–30000	475.5	1349–1236	96	0.09	[36]
1-octyl-3-methylimidazolium bis[(trifluoromethyl)sulfonyl]imide	[omim] [Tf2N]	$C_{14}H_{23}N_3F_6S_2O_4$	298–343	101	475.5	1325–1285	10	0.45	[67]
1-decyl-3-methylimidazolium tetrafluoroborate	[C10mim] [BF4]	$C_{14}H_{27}N_2BF_4$	293	101	310.2	1072	1	2.39	[68]
1-decyl-3-methylimidazolium tetrafluoroborate	[C10mim] [BF4]	$C_{14}H_{27}N_2BF_4$	298	101	310.2	1040	1	0.21	[39]
1-(3-phenylalkyl)-3-methylimidazolium bis[(trifluoromethyl) sulfonyl] imide	[Ph(CH2)3mim] [Tf2N]	$C_{15}H_{17}N_3F_6S_2O_4$	298	101	481.4	1455	1	0.06	[50]
[C3(mim)2] bis[(trifluoromethyl)sulfonyl]imide	[C3(mim)2] [dTf2N]	$C_{15}H_{18}N_6F_{12}S_4O_8$	298	101	766.6	1610	1	0.56	[69]
1-butyl-3-methylimidazolium bis(2-methyllactato)borate	[bmim] [BMLB]	$C_{16}H_{27}N_2O_6B$	298	101	354.2	1143	1	0.01	[63]
1-decyl-3-methylimidazolium bis[(trifluoromethyl)sulfonyl]imide	[C10mim] [Tf2N]	$C_{16}H_{27}N_3F_6S_2O_4$	293	101	503.5	1279	1	1.55	[68]
1-decyl-3-methylimidazolium bis[(trifluoromethyl)sulfonyl]imide	[C10mim] [Tf2N]	$C_{16}H_{27}N_3F_6S_2O_4$	298	101	503.5	1271	1	1.88	[39]
1-butyl-3-methylimidazolium octyl sulfate	[bmim] [C8S]	$C_{16}H_{32}N_2SO_4$	278–328	101	348.5	1000–986	6	0.54	[70]
[C9(mim)2] bromide	[C9(mim)2] [dBr]	$C_{17}H_{30}N_4Br_2$	298	101	450.3	1410	1	0.51	[69]
[C6(mim)2] bis[(trifluoromethyl)sulfonyl]imide	[C6(mim)2] [dTf2N]	$C_{18}H_{24}N_6F_{12}S_4O_8$	298	101	808.7	1520	1	0.03	[69]

Table 2 Continued

IUPAC name	Abbreviation	Formula	T (K)	P (kPa)	M	ρ (kg · m^{-3})	No. data	*AARD*	Ref.
1-dodecyl-3-ethylimidazolium trifluoromethanesulfonate	[C10eim] [TfO]	$C_{18}H_{31}N_2F_3SO_3$	298	101	414.5	1100	1	3.80	[33]
1-dodecyl-3-methylimidazolium bis[(trifluoromethyl)sulfonyl]imide	[C12mim] [Tf2N]	$C_{18}H_{31}N_3F_6S_2O_4$	293	101	531.6	1246	1	0.92	[68]
1-dodecyl-3-methylimidazolium 1,1,2,2-tetrafluoroethanesulfonate	[C12mim] [TFES]	$C_{18}H_{32}N_2F_4SO_3$	301	101	432.5	1136	1	0.18	[33]
[C12(mim)2] tetrafluoroborate	[C12(mim)2] [dBF4]	$C_{20}H_{36}N_4B_2F_8$	298	101	506.1	1260	1	0.21	[69]
[C12(mim)2] hexafluorophosphate	[C12(mim)2] [dPF6]	$C_{20}H_{36}N_4P_2F_{12}$	298	101	622.5	1360	1	0.27	[69]
[C9(mim)2] bis[(trifluoromethyl)sulfonyl]imide	[C9(mim)2] [dTf2N]	$C_{21}H_{30}N_6F_{12}S_4O_8$	298	101	850.8	1470	1	0.46	[69]
1-butyl-3-methylimidazolium bis(salicylato)borate	[bmim] [BScB]	$C_{22}H_{23}N_2O_6B$	298	101	422.2	1311	1	0.00	[63]
[C9(bim)2] bromide	[C9(bim)2] [dBr]	$C_{23}H_{42}N_4Br_2$	298	101	534.4	1270	1	0.07	[69]
[C9(bim)2] tetrafluoroborate	[C9(bim)2] [dBF4]	$C_{23}H_{42}N_6B_2F_8$	298	101	548.2	1200	1	0.19	[69]
[C12(mim)2] bis[(trifluoromethyl)sulfonyl]imide	[C12(mim)2] [dTf2N]	$C_{24}H_{36}N_6F_{12}S_4O_8$	298	101	892.8	1400	1	0.83	[69]
[C9(bim)2] bis[(trifluoromethyl)sulfonyl]imide	[C9(bim)2] [dTf2N]	$C_{27}H_{42}N_6F_{12}S_4O_8$	298	101	934.9	1350	1	2.19	[69]
Prediction Set									
1-methyl-3-methylimidazolium tetrachloroaluminate	[mmim] [AlCl4]	$C_5H_9N_2AlCl_4$	298	101	265.9	1329	1	0.21	[38]
1-methyl-3-methylimidazolium chloride	[mmim] [Cl]	$C_5H_9N_2Cl$	298	101	132.6	1140	1	4.90	[39]
1-ethyl-3-methylimidazolium methylsulfonate	[emim] [MsO]	$C_7H_{14}N_2SO_3$	298	101	206.3	1244	1	0.21	[42]
1-butyl-3-methylimidazolium bromide	[bmim] [Br]	$C_8H_{15}N_2Br$	298–323	101	219.1	1299–1284	6	0.18	[5]

Table 2 Continued

IUPAC name	Abbreviation	Formula	T (K)	P (kPa)	M	ρ (kg · m^{-3})	No. data	*AARD*	Ref.
1-metoxyethyl-3-methylimidazolium bis[(trifluoromethyl)sulfonyl]imide	[moemim] [Tf2N]	$C_9H_{13}N_3F_6S_2O_4$	293	101	421.3	1500	1	0.48	[68]
1-ethyl-3,5-dimethylimidazolium bis[(trifluoromethyl)sulfonyl]imide	[eDmim] [Tf2N]	$C_9H_{13}N_3F_6S_2O_4$	295	101	405.3	1470	1	1.18	[33]
1-metoxyethyl-3-methylimidazolium bis[(trifluoromethyl)sulfonyl]imide	[moemim] [Tf2N]	$C_9H_{13}N_3F_6S_2O_4$	295	101	421.3	1496	1	0.60	[33]
1-butyl-3-methylimidazolium trifluoromethanesulfonate	[bmim] [TfO]	$C_9H_{15}N_2F_3SO_3$	298	101	288.3	1298	1	0.91	[33]
1-butyl-3-methylimidazolium trifluoromethanesulfonate	[bmim] [TfO]	$C_9H_{15}N_2F_3SO_3$	296–343	101	288.3	1301–1270	5	0.49	[60]
dimethyl-3-ethylimidazolium bis[(trifluoromethyl)sulfonyl]imide	[dmeim] [Tf2N]	$C_9H_{16}N_3F_6S_2O_4$	298	101	405.3	1480	1	0.34	[33]
1-[2-(2-methoxyethoxy)ethyl]-3-methylimidazolium tetrafluoroborate	[moeoemim] [BF4]	$C_9H_{17}N_2O_2BF_4$	298	101	272.1	1220	1	0.46	[39]
1-butyl-2,3-dimethylimidazolium hexafluorophosphate	[bdmim] [PF6]	$C_9H_{17}N_2PF_6$	313–393	100–10000	298.2	1345–1276	63	1.69	[1]
1-butyl-2,3-dimethylimidazolium hexafluorophosphate	[bdmim] [PF6]	$C_9H_{17}N_2PF_6$	296–323	101	298.2	1242–1206	3	5.67	[60]
1-ethyl-3-methylimidazolium 1-carbon icosahedral	[emim] [CB11H12]	$C_9H_{23}N_2B_{11}$	298	101	254.2	1067	1	0.02	[43]
5-methyl-1,3-diethylimidazolium bis[(trifluoromethyl)sulfonyl]imide	[mdeim] [Tf2N]	$C_{10}H_{15}N_3F_6S_2O_4$	295	101	419.4	1432	1	1.74	[33]
1-hexyl-3-methylimidazolium chlorogallate	[hmim] [GaCl4]	$C_{10}H_{19}N_2AlCl_4$	308–338	101	378.8	1338–1313	7	0.26	[71]
1-hexyl-3-methylimidazolium indium choride	[hmim] [InCl4]	$C_{10}H_{19}N_2InCl_4$	283–338	101	423.9	1492–1439	12	0.05	[48]
1-hexyl-3-methylimidazolium hexafluorophosphate	[hmim] [PF6]	$C_{10}H_{19}N_2PF_6$	293–393	100–10000	312.2	1305–1219	77	0.18	[1]
1-hexyl-3-methylimidazolium hexafluorophosphate	[hmim] [PF6]	$C_{10}H_{19}N_2PF_6$	278–318	101	312.2	1310–1277	9	0.21	[5]

Table 2 Continued

IUPAC name	Abbreviation	Formula	T (K)	P (kPa)	M	ρ (kg · m^{-3})	No. data	*AARD*	Ref.
1-hexyl-3-methylimidazolium hexafluorophosphate	[hmim] [PF6]	$C_{10}H_{19}N_2PF_6$	293–303	101	312.2	1298–1290	3	0.20	[40]
1-hexyl-3-methylimidazolium hexafluorophosphate	[hmim] [PF6]	$C_{10}H_{19}N_2PF_6$	273–363	101	312.2	1313–1243	14	0.17	[65]
1-hexyl-3-methylimidazolium hexafluorophosphate	[hmim] [PF6]	$C_{10}H_{19}N_2PF_6$	293–303	101	312.2	1298–1290	3	0.20	[5]
1-butyl-3-ethylimidazolium methylsulfonate	[beim] [MsO]	$C_{10}H_{20}N_2SO_3$	298	101	248.3	1140	1	3.17	[33]
1-butyl-3-ethylimidazolium trifluoroacetate	[beim] [ta]	$C_{11}H_{17}N_2F_3O_2$	295	101	266.3	1183	1	0.66	[33]
1-butyl-3-ethylimidazolium bis[(trifluoromethyl)sulfonyl]imide	[beim] [Tf2N]	$C_{11}H_{17}N_3F_6S_2O_4$	295	101	433.4	1404	1	0.08	[33]
1,3-dibutylimidazolium tetrachloroaluminate	[C4C4I] [AlCl4]	$C_{11}H_{21}N_2AlCl4$	298	101	350.1	1164	1	0.05	[38]
1-(4-methoxyphenyl)-3-methylimidazolium trifluoromethanesulfonate	[mpmi] [TfO]	$C_{12}H_{13}N_2F_3SO_4$	323	101	338.3	1320	1	0.01	[33]
1-ethyl-3-methylimidazolium heptafluorobutanoate	[emim] [hb]	$C1_2H_{15}N_2F_7O_2$	295	101	324.2	1450	1	0.35	[33]
1,2-dimethyl-3-propylimidazolium tris(trifluoromethylsulfonyl)methide	[dmpim] [TMEM]	$C_{12}H_{15}N_2F_9S_3O_6$	283–348	101	550.4	1612–1567	4	0.36	[64]
1-butyl-3-methylimidazolium bis(pentafluoroethylsulfonyl)imide	[bmim] [BEI]	$C_{12}H_{15}N_3F_{10}S_2O_4$	288–313	101	505.4	1524–1498	6	0.04	[72]
1-hexyl-3-methylimidazolium bis[(trifluoromethyl)sulfonyl]imide	[hmim] [Tf2N]	$C_{12}H_{19}N_3F_6S_2O_4$	291–307	101	447.4	1378–1364	9	0.13	[5]
1-hexyl-3-methylimidazolium bis[(trifluoromethyl)sulfonyl]imide	[hmim] [Tf2N]	$C_{12}H_{19}N_3F_6S_2O_4$	293–358	101	447.4	1374–1315	14	0.44	[67]
1-hexyl-3-methylimidazolium bis[(trifluoromethyl)sulfonyl]imide	[hmim] [Tf2N]	$C_{12}H_{19}N_3F_6S_2O_4$	298–333	100–59590	447.4	1410–1338	163	0.20	[59]

Table 2 Continued

IUPAC name	Abbreviation	Formula	T (K)	P (kPa)	M	ρ (kg · m^{-3})	No. data	*AARD*	Ref.
1,3-dibutylimidazolium trifluoromethanesulfonate	[dbim] [TfO]	$C_{12}H_{21}N_2F_3SO_3$	303	101	330.4	1300	1	4.19	[33]
1-butyl-3-ethylimidazolium nonafluorobutanesulfonate	[beim] [NfO]	$C_{13}H_{17}N_2F_9SO_3$	295	101	452.3	1427	1	1.39	[33]
1-heptyl-3-methylimidazolium 1,1,2,2-tetrafluoroethanesulfonate	[hpmim] [TFES]	$C_{13}H_{22}N_2F_4SO_3$	301	101	362.4	1274	1	0.35	[33]
1-octyl-3-methylimidazolium dicyanamide	[omim] [dca]	$C_{14}H_{23}N_5$	298	101	261.4	1000	1	0.57	[66]
1-octyl-3-propylimidazolium hexafluorophosphate	[oprim] [PF6]	$C_{14}H_{27}N_2PF_6$	298	101	368.3	1118	1	3.83	[39]
1-nonyl-3-methylimidazolium bis[(trifluoromethyl)sulfonyl]imide	[nmim] [Tf2N]	$C_{15}H_{25}N_3F_6S_2O_4$	298	101	489.5	1299	1	0.77	[39]
1-octyl-3-methylimidazolium nonafluorobutanesulfonate	[omim] [NfO]	$C_{16}H_{23}N_2F_9SO_3$	298	101	494.4	1330	1	0.08	[66]
[C12(mim)2] bromide	[C12(mim)2] [dBr]	$C_{20}H_{36}N_4Br_2$	298	101	492.3	1270	1	0.49	[69]
[C9(m2im)2] bis[(trifluoromethyl)sulfonyl]imide	[C9(m2im)2] [dTf2N]	$C_{23}H_{36}N_6F_{12}S_4O_8$	298	101	880.8	1470	1	0.30	[69]
[C9(bim)2] hexafluorophosphate	[C9(bim)2] [dPF6]	$C_{23}H_{42}N_4P_2F_{12}$	298	101	664.5	1300	1	0.46	[69]
[C12(benzim)2] hexafluorophosphate	[C12(benzim)2] [dPF6]	$C_{32}H_{44}P_2F_{12}$	298	101	774.7	1270	1	0.01	[69]

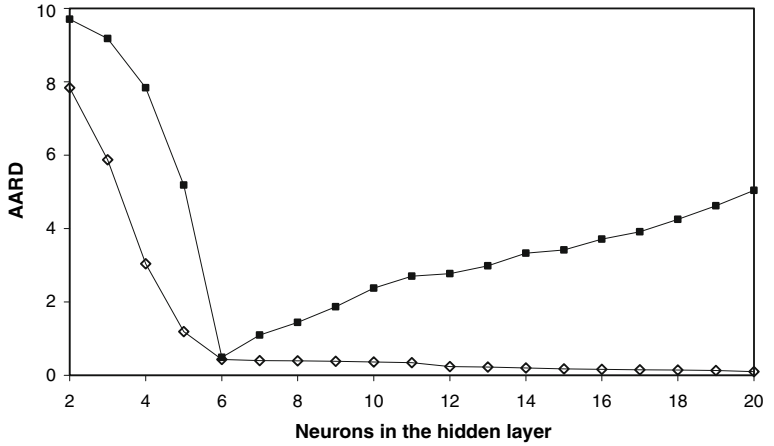

Fig. 2 Average absolute deviation (in %) found in correlating the liquid density of all ILs as a function of the number of neurons in the hidden layer: (◊) during training and (■) during prediction

Table 3 Overall minimum, maximum, and average deviations for the calculated liquid density for all MIM-ILs using the ANN + PSO model

ANN model	Training set	Prediction set	Total set
Experimental data			
No. ionic liquids	131	33	164
No. data points	1736	426	2162
Deviations			
$AARD_{\min}$ (%)	0.00	0.00	0.00
$AARD_{\max}$ (%)	6.58	6.51	6.58
AARD (%)	0.43	0.49	0.44
No. $AARD < 5\,\%$	1732	424	2156
No. $AARD > 10\,\%$	0	0	0

4 Results and Discussion

Table 2 presents the results of the method for each ionic liquid used in this study. The last column in the table shows these deviations. The results were calculated using Eq. 7. Also shown at the end of Table 2 are the deviations for the 33 MIM-ILs used to check the prediction capabilities of the trained network. As observed in the table, the deviations for these ILs are within the same ranges found during training.

Table 3 shows the overall minimum, maximum, and average deviations calculated by Eq. 7, for all MIM-ILs using the proposed network 33-6-1. The results show that the ANN + PSO model can be accurately trained and that the chosen topology can estimate the liquid density of ILs at several temperatures and pressures with accuracy and give lower deviations than other models available in the literature ($AARD$ less than 0.43 % for the 1736 data points used in the training and $AARD$ less than 0.49 % for

Table 4 Optimum weight and biases for the ANN 33-6-1

Input	w_1	1	2	3	4	5	6
T (K)	1	0.4628	0.2631	0.3654	0.4712	0.4168	0.0126
P (kPa)	2	−1.2532	−0.5468	−0.7770	−1.2951	−1.1447	0.0452
M	3	−1.5742	−1.0731	0.6360	−0.9130	0.2144	−0.2154
–CH_3	4	−0.7404	0.2173	−2.0378	−1.1929	−2.3124	−0.2181
–CH_2–	5	−2.9001	−0.0164	−2.3218	−3.2172	−5.8168	0.1720
>CH–	6	−0.0182	0.2022	−0.1040	−0.0048	0.1822	−0.2081
>C<	7	−0.0920	0.2367	−0.3520	−0.2229	−0.5341	−0.1508
–OH	8	0.2387	−0.2235	0.0906	0.2595	0.1500	0.2540
–O–	9	−0.0129	0.0702	0.4677	0.0104	0.7799	0.1391
–COO–	10	−1.1049	−0.3481	−0.1979	−0.7036	1.6544	0.1315
>N–	11	0.2865	0.6445	1.9268	−0.2154	0.7301	1.1587
–CN	12	−0.9153	0.1206	0.3014	−0.7829	−0.1732	0.0613
–NO_2	13	0.7113	−0.0057	−0.4281	0.3568	0.3676	−0.1794
–F	14	0.4542	−0.0812	0.4305	0.4198	0.8333	0.1180
–Cl	15	0.3853	0.3370	−0.4736	0.3573	1.1915	−0.0223
–Br	16	0.2433	−1.1714	0.0106	0.4393	0.6094	0.1011
–P	17	0.6005	0.5496	0.0162	0.5828	0.9064	−0.4704
–B	18	0.5427	0.2680	−0.7818	0.5047	2.5040	−0.2106
–S–	19	−0.1175	0.2942	−0.7969	−0.2307	0.1382	−0.2808
–SO_2–	20	−0.4012	−0.1745	0.2348	−0.3069	2.0618	0.0902
=CH–	21	0.8832	1.3496	0.9699	0.2236	−0.4437	−0.3323
>C<	22	−0.3491	−0.1937	0.1637	−0.4709	−0.1681	0.0281
=C<	23	−1.8068	−0.7329	−0.0061	−1.5351	−1.3384	0.2518
–O–	24	0.1711	−0.6106	−0.1732	0.9701	−0.2492	−0.2290
>C=O	25	0.4850	0.3449	−0.5231	0.2743	−0.2692	0.0477
–NH–	26	0.4350	0.1869	0.0821	0.0126	−0.2680	0.0330
>N–	27	1.5526	−0.1628	0.8947	1.7112	0.2855	0.1521
=N–	28	0.1674	0.1110	0.6783	0.1777	0.1799	0.3369
–BH	29	0.1240	0.1353	0.0419	−0.0209	0.6915	0.3579
–Al	30	0.3208	−0.3135	−0.7804	0.4159	−0.7273	−0.2415
–Ga	31	0.8353	0.1490	0.3629	0.5388	−0.2831	−0.2346
–In	32	0.8616	0.1096	0.3347	0.6140	−0.1089	−0.2753
–Fe	33	0.4424	−0.4519	0.2938	0.0898	−0.1356	0.3013
	b_1	1.1084	−1.1960	−0.0851	−0.0847	−0.9165	1.1919
w_2	1	2	3	4	5	6	b_2
1	1.0632	−0.6390	0.4625	−1.1806	0.4432	−1.1644	0.3743

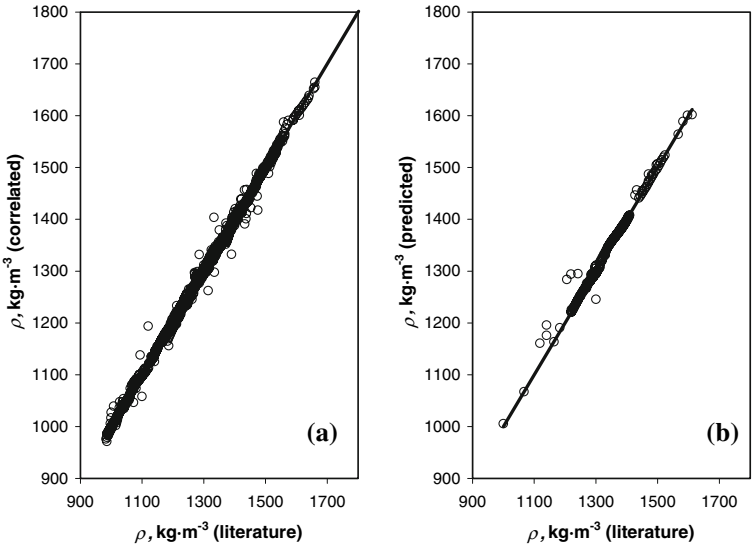

Fig. 3 Comparison between experimental and calculated values of liquid density of MIM-ILs: **a** during training and **b** during prediction

the 462 data points in the prediction step). For all data (2162 data points) the $AARD$ is below 10 %, and for 2156 data points, the $AARD$ is below 5 %.

Note that these deviations are relatively small if one considers the deviations between some experimental data published in the open literature. Valderrama and co-authors [33] show the experimental densities that have been published by different authors for two ionic liquids. Deviations up to 17 % are observed between some values.

Once the architecture was determined, the optimum weights required to carry out the estimate of $\rho(T, P)$ for any MIM-ILs were obtained. Table 4 shows the optimum weight and bias for the ANN 33-6-1.

Figure 3 shows a comparison between experimental (solid line) and calculated values (circles) by the ANN + PSO model to determine $\rho(T, P)$. Figure 3a shows a comparison during training between correlated and literature values of the liquid density. The correlation coefficient R^2 is 0.9947. Figure 3b shows a comparison during prediction between predicted and literature values of ρ for MIM-ILs. In this case, the correlation coefficient R^2 is 0.9883. For the total set, R^2 is 0.9934. The figure ratifies the discussion presented above.

5 Conclusions

In this work, the liquid density of imidazolium-based ionic liquids ILs as a function of temperature and pressure has been correlated and predicted using a simple group contribution method implemented in an artificial neural network replacing the standard backpropagation algorithm with particle swarm optimization.

Based on the results and discussion presented in this study, the following main conclusions are obtained: (i) The great differences in the structure and the chemical and physical properties of the MIM-ILs considered in the study impose additional difficulties to the problem that the proposed ANN + PSO model has been able to handle; (ii) The results show that the ANN + PSO model can be properly trained and that the chosen topology (33-6-1) can estimate the liquid density for MIM-ILs at several temperatures and pressures with accuracy and with deviations within experimental errors; (iii) The values calculated with the proposed method are believed to be accurate enough for engineering calculations, for generalized correlations, and for equation-of-state methods, among other uses.

References

1. R.L. Gardas, M.G. Freire, P.J. Carvalho, I.M. Marrucho, I.M.A. Fonseca, A.G.M. Ferreira, J.A.P. Coutinho, J. Chem. Eng. Data **52**, 80 (2007)
2. K.R. Seddon, Kinetics Catal. **37**, 693 (1996)
3. H. Zhao, S.V. Malhotra, Aldrichim. Acta **35**, 75 (2002)
4. Y.U. Paulechka, G.J. Kabo, A.V. Blokhin, A.S. Shaplov, E.I. Lozinskaya, Y.S. Vygodskii, J. Chem. Thermodyn. **39**, 158 (2007)
5. J.A. Lazzús, J. Taiwan Inst. Chem. Eng. **40**, 213 (2009)
6. J. Palomar, V.R. Ferro, J.S. Tordecilla, F. Rodríguez, Ind. Eng. Chem. Res. **46**, 6041 (2009)
7. R.A. Mantz, P.C. Trulove, in *Ionic Liquids in Synthesis*, ed. by P. Wasserscheid, T. Welton (Wiley-VCH Verlag GmbH and Co. KGaA, Germany, 2002), pp. 56–126
8. J.M.S.S. Esperança, H.J.R. Guedes, M. Blesic, L.P.N. Rebelo, J. Chem. Eng. Data **51**, 237 (2006)
9. R.L. Gardas, J.A.P. Coutinho, Fluid Phase Equilib. **263**, 26 (2008)
10. J.O. Valderrama, J.A. Lazzús, K. Zarricueta, in *Proceedings of 2nd Internacional Symposium on Biothermodynamics* (Frankfurt, Germany, 2008)
11. A.L. Lydersen, *Estimation of Critical Properties of Organic Compounds* (Univ. Wisconsin Coll. Eng., Eng. Exp. Stn. Rep. 3, Wisconsin, 1955)
12. K. Joback, R. Reid, Chem. Eng. Commun. **57**, 233 (1987)
13. G.M. Tarver, J. Chem. Eng. Data **24**, 136 (1979)
14. H.S. Elbro, A. Fredenslund, P. Rasmussen, Ind. Eng. Chem. Res. **30**, 2576 (1991)
15. H.L. Ammon, S. Mitchell, Propell. Explos. Pyrotech. **23**, 260 (1998)
16. H.L. Ammon, Struct. Chem. **12**, 205 (2001)
17. E.C. Ihmels, J. Gmehling, Ind. Eng. Chem. Res. **42**, 408 (2003)
18. E. Stefanis, L. Constantinou, I. Tsivintzelis, C. Panayiotou, Int. J. Thermophys. **26**, 1369 (2005)
19. C. Ye, J.M. Shreeve, J. Phys. Chem. A **111**, 1456 (2007)
20. M.T. Hagan, H.B. Demuth, M. Beal, *Neural Network Design* (PWS Publishing Company, Boston, 1996)
21. J.A. Lazzús, Chin. J. Chem. Phys. **22**, 19 (2009)
22. J. Taskinen, J. Yliruusi, Adv. Drug Deliver. Rev. **55**, 1163 (2003)
23. A. Sözen, M. Özalp, E. Arcaklio, Chem. Eng. Process. **43**, 1253 (2004)
24. J.A. Lazzús, Thermochim. Acta **489**, 53 (2009)
25. Q. Luo, D. Yi, Appl. Math. Comput. **199**, 611 (2008)
26. J. Tettech, E. Metcalfe, S.L. Howells, Chemom. Intell. Lab. Syst. **32**, 177 (1996)
27. G. Espinosa, D. Yaffe, A. Arenas, Y. Cohen, F. Giralt, Ind. Eng. Chem. Res. **40**, 2757 (2001)
28. D. Yaffe, Y. Cohen, J. Chem. Inf. Comput. Sci. **41**, 463 (2001)
29. MATLAB Version 6.5.0, The MathWorks Inc
30. R.C. Eberhart, J. Kennedy, in *Proceedings of 6th International Symposium on Micro Machine and Human Science* (Nagoya, Japan, 1995), pp. 39–43
31. Y. Da, G. Xiurun, Neurocomputing **63**, 527 (2005)
32. Y. Jiang, T. Hu, C.-C. Huang, X. Wu, Appl. Math. Comput. **193**, 231 (2007)
33. J.O. Valderrama, W.W. Sanga, J.A. Lazzús, Ind. Eng. Chem. Res. **47**, 1318 (2008)
34. P.-Y. Chen, C.L. Hussey, Electrochim. Acta **49**, 5125 (2004)

35. P. Navia, J. Troncoso, L. Romani, J. Chem. Eng. Data **52**, 1369 (2007)
36. R.L. Gardas, M.G. Freire, P.J. Carvalho, I.M. Marrucho, I.M.A. Fonseca, A.G.M. Ferreira, J.A.P. Coutinho, J. Chem. Eng. Data **51**, 1881 (2007)
37. J.-Z. Yang, Q.-G. Zhang, F. Xue, J. Mol. Liq. **128**, 81 (2006)
38. S.-L. Zang, Q.-G. Zhang, M. Huang, B. Wang, J.-Z. Yang, Fluid Phase Equilib. **230**, 192 (2005)
39. S. Zhang, N. Sun, X. He, X. Lu, X. Zhang, J. Phys. Chem. Ref. Data **35**, 1475 (2006)
40. A.B. Pereiro, J.L. Legido, A. Rodríguez, J. Chem. Thermodyn. **39**, 1168 (2007)
41. A.B. Pereiro, F.P. Santamarta, E. Tojo, A. Rodríguez, J. Tojo, J. Chem. Eng. Data **51**, 952 (2006)
42. A. Arce, E. Rodríguez, A. Soto, Fluid Phase Equilib. **242**, 164 (2006)
43. A.S. Larsen, J.D. Holbrey, F.S. Tham, C.A. Reed, J. Am. Chem. Soc. **122**, 7264 (2000)
44. S. Carda-Broch, A. Berthod, D.W. Armstrong, Anal. Bioanal. Chem. **375**, 191 (2003)
45. L.P.N. Rebelo, V. Najdanovic-Visak, Z.P. Visak, M. Nunes da Ponte, J. Szydlowski, C.A. Cerdeiriña, J. Troncoso, L. Romaní, J.M.S.S. Esperança, H.J.R. Guedes, H.C. de Sousa, Green Chem. **6**, 396 (2004)
46. Y.A. Sanmamed, D. González-Salgado, J. Troncoso, C.A. Cerdeiriña, L. Romaní, Fluid Phase Equilib. **252**, 96 (2007)
47. Q.-G. Zhang, J.-Z. Yang, X.-M. Lu, J.-S. Gui, M. Huang, Fluid Phase Equilib. **226**, 207 (2004)
48. J. Tong, Q.-S. Liu, P. Zhang, J.-Z. Yang, J. Chem. Eng. Data **52**, 1497 (2007)
49. L.A. Blanchard, Z. Gu, J.F. Brennecke, J. Phys. Chem. B **105**, 2437 (2001)
50. S.V. Dzyuba, R.A. Bartsch, Chem. Phys. Chem. **3**, 161 (2002)
51. A.B. Pereiro, P. Verdía, E. Tojo, A. Rodríguez, J. Chem. Eng. Data **52**, 377 (2007)
52. J. Troncoso, C.A. Cerdeiriña, Y.A. Sanmamed, L. Romaní, L.P.N. Rebelo, J. Chem. Eng. Data **51**, 1856 (2006)
53. Z. Gu, J.F. Brennecke, J. Chem. Eng. Data **47**, 339 (2002)
54. E. Gómez, B. González, N. Calvar, E. Tojo, A. Domínguez, J. Chem. Eng. Data **51**, 2096 (2006)
55. H. Rodriguez, J.F. Brennecke, J. Chem. Eng. Data **51**, 2145 (2006)
56. J. Tong, M. Hong, W. Guan, J.-B. Li, J.-Z. Yang, J. Chem. Thermodyn. **38**, 1416 (2006)
57. D. Xiao, J.R. Rajian, A. Cady, S. Li, R.A. Bartsch, E.L. Quitevis, J. Phys. Chem. B **111**, 4669 (2007)
58. M.B. Shiflett, M.A. Harmer, C.P. Junk, A. Yokozeki, Fluid Phase Equilib. **242**, 220 (2006)
59. R. Gomes de Azevedo, J.M.S.S. Esperança, J. Szydlowski, Z.P. Visak, P.F. Pires, H.J.R. Guedes, L.P.N. Rebelo, J. Chem. Thermodyn. **37**, 888 (2005)
60. C.P. Fredlake, J.M. Crosthwaite, D.G. Hert, S.N.V.K. Aki, J.F. Brennecke, J. Chem. Eng. Data **49**, 954 (2004)
61. E. Gómez, B. González, A. Domínguez, E. Tojo, J. Tojo, J. Chem. Eng. Data **51**, 696 (2006)
62. J.M.S.S. Esperança, Z.P. Visak, N.V. Plechkova, K.R. Seddon, H.J.R. Guedes, L.P.N. Rebelo, J. Chem. Eng. Data **51**, 2009 (2006)
63. W. Xu, L.-M. Wang, R.A. Nieman, C.A. Angell, J. Phys. Chem. B **107**, 11749 (2003)
64. M.B. Shiflett, M.A. Harmer, C.P. Junk, A. Yokozeki, J. Chem. Eng. Data **51**, 483 (2006)
65. K.R. Harris, M. Kanakubo, L.A. Woolf, J. Chem. Eng. Data **52**, 1080 (2007)
66. N. Papaiconomou, N. Yakelis, J. Salminen, R. Bergman, J.M. Prausnitz, J. Chem. Eng. Data **51**, 1389 (2006)
67. R. Kato, J. Gmehling, J. Chem. Thermodyn. **37**, 603 (2005)
68. L. Glasser, Thermochim. Acta **421**, 87 (2004)
69. J.L. Anderson, R. Ding, A. Ellern, D.W. Armstrong, J. Am. Chem. Soc. **127**, 593 (2005)
70. A.V. Orchillés, V. González-Alfaro, P.J. Miguel, E. Vercher, A. Martínez-Andreu, J. Chem. Thermodyn. **38**, 1124 (2006)
71. J. Tong, Q.-S. Liu, W. Guan, J.-Z. Yang, J. Phys. Chem. B **111**, 3197 (2007)
72. H. Tokuda, S. Tsuzuki, M.A.B.H. Susan, K. Hayamizu, M. Watanabe, J. Phys. Chem. B **110**, 19593 (2006)